

Transverse-momentum spectra of strange particles produced in Pb+Pb collisions at $\sqrt{s_{\text{NN}}} = 2.76$ TeV in the chemical non-equilibrium model

Viktor Begun,^{1,2} Wojciech Florkowski,^{1,3} and Maciej Rybczynski¹

¹*Institute of Physics, Jan Kochanowski University, PL-25406 Kielce, Poland*

²*Bogolyubov Institute for Theoretical Physics, 03680 Kiev, Ukraine*

³*The H. Niewodniczański Institute of Nuclear Physics,
Polish Academy of Sciences, PL-31342 Kraków, Poland*

(Dated: May 27, 2014)

Abstract

We analyze the transverse-momentum spectra of strange hadrons produced in Pb+Pb collisions at the collision energy $\sqrt{s_{\text{NN}}} = 2.76$ TeV. Our approach combines the concept of chemical non-equilibrium with the single-freeze-out scenario. The two ideas are realized in the framework of the Cracow model, whose thermodynamic parameters have been established in earlier studies of the ratios of hadron multiplicities. The geometric parameters of the model are obtained from the fit to the spectra of pions and kaons, only. Using these parameters, we obtain an excellent description of the spectra of protons and the K_S^0 , $K^*(892)^0$, and $\phi(1020)$ mesons. A satisfactory description is also obtained for the Λ , Ξ and Ω hyperons. Further improvement of the hyperon spectra may be achieved if we assume that they are emitted from a smaller, internal part of the system but at the same thermodynamic conditions. Our work not only includes all particle species measured up to now in heavy-ion collisions at the LHC energies but, in addition, discusses the centrality dependence of the particle production.

PACS numbers: 25.75.-q, 25.75.Dw, 25.75.Ld

Keywords: relativistic heavy-ion collisions, thermal models of hadron production, statistical hadronization, Relativistic Heavy Ion Collider (RHIC), Large Hadron Collider (LHC)

I. INTRODUCTION

Thermal and statistical models of hadron production [1–18, 20] have become the standard tools to analyze mean multiplicities of the particles produced in heavy-ion collisions. They have explained successfully the AGS [5–7], SPS [8–14], and RHIC [15–20] data on hadronic abundances. Supplemented by the proper definition of the spacetime geometry and hydrodynamic flow at freeze-out, the statistical models allow us to describe the transverse-momentum spectra and other soft-hadronic observables [17–21]. Nevertheless, the recent LHC data on heavy-ion collisions show that the predictions of two popular versions of the statistical model (the chemical equilibrium model and the strangeness non-equilibrium model) give too large values for the kaon to pion ratio, $(K^+ + K^-)/(\pi^+ + \pi^-)$, and, especially, for the ratio of protons to pions $(p + \bar{p})/(\pi^+ + \pi^-)$ [22, 23]. The recent fit [24] gives almost three standard deviations higher values for protons and anti-protons compared to the LHC data.

The pions, kaons and protons are the most abundant particles that are produced in heavy-ion collisions, therefore, this discrepancy is very uncomfortable for the thermal interpretation of hadron production. The problem with the correct description of protons is sometimes referred to as the *proton puzzle* [25].

There have been two solutions to this puzzle proposed up to now. The first one is to use the UrQMD model to calculate the modification factors for each particle and then to use these factors in the equilibrium statistical model to account for possible discrepancies [26, 27]. A clear disadvantage of this approach is that adding a hadronic afterburner to a thermal model spoils the natural simplicity of the latter — the main aim of introducing thermal models was to gain a simple description of hadron production which does not refer directly to the aspects of microscopic dynamics. Nevertheless, using the kinetic model one can successfully attribute the modification factors to the baryon-antibaryon annihilation and other microscopic mechanisms which are taken into account by the UrQMD simulations.

The second solution to the proton puzzle has been achieved by assuming that statistical hadronization happens out of chemical equilibrium [28, 29]. An advantage of this approach is that it continues to use simple concepts of thermal approach not invoking directly to kinetic simulations. The mean multiplicities are explained by adding only two non-equilibrium parameters, γ_q and γ_s (the hadron abundances scale with γ_q and γ_s depending on the number of the constituent light and strange quarks within a hadron). It is worth mentioning that the chemical non-equilibrium approach offers also a possibility to calculate the modification factors

studied within the UrQMD approach and to interpret them in terms of the non-equilibrium parameters. Such a calculation may form a link between two alternative explanations of the data.

Besides the problems with thermal interpretation of the hadron abundances at the LHC, one encounters also the problems with the hydrodynamic interpretation of the transverse-momentum spectra of pions, kaons and protons, see Fig. 1 in Ref. [22] and Figs. 13, 14, 15 of Ref. [23]. The ratios data/model analyzed in Ref. [23] have a very characteristic convex shape. Quite a few hydrodynamic models are discussed in [23]: VISH2+1 [30], HKM [31], EPOS [32] and Krakow [33]¹. All these models exhibit a deficit in the very low- p_T region, with the largest effect of about 25–50% for pions in the most central collisions ($c = 0$ –5%). In the ultra-peripheral collisions ($c = 70$ –80%), the models fail to reproduce the data at both the low and high transverse momenta. Similar features appear in the calculations presented in Refs. [34] and [35]. This situation is quite surprising, as the hydrodynamic models are supposed to work at low momenta, let us say up to $p_T \sim 2$ GeV.

In our earlier paper [36], we have shown that one can connect the proton puzzle with the anomalous behavior of the pion p_T spectra and solve the two problems within the chemical non-equilibrium version of the Cracow single freeze-out model. Encouraged by the success of our approach, in this paper we extend our study to all measured hadrons including the recently measured strange mesons and baryons. Following the same procedure as in [36], we take the values of *thermodynamic* parameters from Ref. [29] and find the model *geometric* parameters from the fit to the pion and kaon spectra, only. In the next step, with the same parameters we determine the spectra of other hadrons. In this work we show that this strategy leads to an excellent description of the spectra of $p + \bar{p}$, K_S^0 , $K^*(892)^0$, and $\phi(1020)$. A satisfactory description is also obtained for Λ , Ξ and Ω . Further improvement of the hyperon spectra may be achieved if we assume that they are emitted from a smaller, internal part of the system but still at the same chemical non-equilibrium thermodynamic conditions.

In [36] we analyzed the p_T spectra of pions, kaons and protons in the most central, $c = 0$ –5%, and semi-peripheral, $c = 30$ –40%, collisions. In this paper we consider all centrality classes from the most central, $c = 0$ –5%, to ultra-peripheral, $c = 80$ –90%, collisions and all particles

¹ We note that the Krakow hydrodynamic model cited in [23] is different from the Cracow freeze-out model used in our paper, although the former uses also the concept of single-freeze-out at the end of the hydrodynamic evolution.

measured by the ALICE collaboration up to now: π , K , p , K_S^0 , Λ , $K^*(892)^0$, $\phi(1020)$, Ξ and Ω [23, 37–39].

The paper is organized as follows: In Sec. II we introduce our approach based on the Monte-Carlo version of the Cracow model as implemented in the **THERMINATOR** code [40, 41]. The parameters of the model are fixed by the fits to the pion and kaon spectra, which are described in Sec. III. The results showing the p_T spectra of strange particles are presented in Sec. IV. The general discussion of our physics results in Section V and the two Appendices close the paper.

II. THE CRACOW MODEL

A. The freeze-out spacetime geometry

The starting point for our considerations is the Cooper-Frye formula. The hadron rapidity and transverse-momentum distributions are calculated from the expression

$$\frac{dN}{dyd^2p_T} = E \frac{dN}{d^3p} = \int d\Sigma \cdot p f(p \cdot u), \quad (1)$$

where $d\Sigma_\mu = \tau_f r dr d\eta d\varphi u_\mu$ is an element of the freeze-out hypersurface and u^μ is the hydrodynamic Hubble-like flow at freeze-out

$$u^\mu = \frac{x^\mu}{\tau_f} = \frac{(t, x, y, z)}{\tau_f}. \quad (2)$$

The parameter τ_f fixes invariant time at freeze-out, $\tau_f^2 = t^2 - x^2 - y^2 - z^2$. Hence, the freeze-out hypersurface may be conveniently parameterized with the help of three variables. In our case we use the transverse distance from the collision axis, $r = \sqrt{x^2 + y^2}$, the spacetime rapidity, $\eta = 1/2 \ln(t + z)/(t - z)$, and the azimuthal angle, $\varphi = \tan^{-1}(y/x)$. Since we consider a boost-invariant system, the integration over the spacetime rapidity η in (1) stretches from minus to plus infinity. On the other hand, the integration over r is restricted to the range $0 \leq r \leq r_{\max}$, where r_{\max} defines the edge of a firecylinder. The quantities τ_f and r_{\max} are the only two geometric parameters of the Cracow model.

The distribution function $f(p \cdot u)$ consists of primordial (directly produced) and secondary (produced by resonance decays) contributions. The decays are handled by **THERMINATOR** [40, 41] and include all particles and well established resonances. The primordial distribution of the i th hadron in the local rest frame has the form [42]

$$f_i(p, T, \Upsilon_i) = \frac{g_i}{\Upsilon_i^{-1} \exp(\sqrt{p^2 + m_i^2}/T) \mp 1}. \quad (3)$$

Here g_i is the degeneracy factor connected with spin, m_i is the mass of the particle, Υ_i is the particle's fugacity, and T is the system's temperature. The -1 ($+1$) sign corresponds to bosons (fermions).

The integration of the distribution function (3) over three-momentum gives the hadron density

$$n_i(T, \Upsilon_i) = \int \frac{d^3p}{(2\pi)^3} f_i(p, T, \Upsilon_i). \quad (4)$$

Similarly, the integration of the distribution (1) over transverse-momentum gives the rapidity distribution dN/dy . In the Appendix A we show that the freeze-out geometry of our model implies the relation ²

$$\frac{dN_i}{dy} = \frac{dN_i}{d\eta} = \pi r_{\text{max}}^2 \tau_f n_i(T, \Upsilon_i). \quad (5)$$

Consequently, the knowledge of the thermodynamic parameters together with the rapidity density allows us to determine the system's volume per unit rapidity

$$\frac{dV}{dy} = \pi r_{\text{max}}^2 \tau_f. \quad (6)$$

As we shall see below, an independent experimental estimate of this quantity may serve us to reduce the number of independent geometric parameters of our model from two to just one.

B. Implementation of the chemical non-equilibrium

The fugacity factor Υ_i is defined as

$$\Upsilon_i = \gamma_q^{N_q^i + N_{\bar{q}}^i} \gamma_s^{N_s^i + N_{\bar{s}}^i} \exp\left(\frac{\mu_Q Q_i + \mu_B B_i + \mu_S S_i}{T}\right), \quad (7)$$

where μ_Q , μ_B , and μ_S are the electric, baryon, and strange chemical potentials in the system, while Q_i , B_i , and S_i are the electric charge, baryon number, and strangeness of the i th hadron [36, 42]. The chemical potentials are very small at the LHC energies. Therefore, for simplicity ³, we set $\mu_Q = \mu_B = \mu_S = 0$ and obtain

$$\Upsilon_i = \gamma_q^{N_q^i + N_{\bar{q}}^i} \gamma_s^{N_s^i + N_{\bar{s}}^i}. \quad (8)$$

² We stress that η denotes the spacetime rapidity in our model, hence, Eq. (5) means that the *spacetime rapidity* distribution is equal to the *rapidity* distribution. On the other hand, the *pseudorapidity* and *rapidity* densities are usually quite different, especially at $y = 0$ [21].

³ This assumption does not affect our results, because we do not consider very small differences between particles and anti-particles at the LHC and analyze only their total number. We also neglect the contributions from the charmed hadrons in Eqs. (7) and (8).

The quantities N_q^i and N_s^i in (7) and (8) are the numbers of light (u, d) and strange (s) quarks in the i th hadron, while $N_{\bar{q}}^i$ and $N_{\bar{s}}^i$ are the numbers of the antiquarks in the same hadron. The γ_q and γ_s parameters account for deviations from chemical equilibrium and affect the mean multiplicities of the particles with (u, d) and (s) quarks, respectively. In this work, similarly to our previous paper [36], we compare two cases: the non-equilibrium statistical hadronization version of the Cracow model (NEQ SHM), where $\gamma_q \neq 1$ and $\gamma_s \neq 1$, and the equilibrium version (EQ SHM), where $\gamma_q = \gamma_s = 1$.

In typical calculations, the use of the parameter γ_s does not lead to substantial modifications of other thermodynamic parameters, like temperature or volume, but helps to describe strange particles. The appearance of γ_s can be explained, for example, in the so called core-corona model [44–47], where a superposition of two sources of particle production is taken into account: single nucleon-nucleon (NN) collisions and a fully equilibrated source.

The use of $\gamma_q > 1$ (to our knowledge, introduced for the first time in [48]) makes the freeze-out temperature and/or volume smaller, because it influences the most abundant particles in the medium: pions are multiplied by γ_q^2 while protons by γ_q^3 . The temperature found in the recent chemical non-equilibrium calculations [29] is about 140 MeV. It is lower than the transition temperature obtained by the Wuppertal-Budapest Collaboration, $T_c = 150\text{--}170$ MeV. We note, however, that direct comparisons of the chemical non-equilibrium models (i.e., the models with $\gamma_s \neq 1$ and/or $\gamma_q \neq 1$) with the lattice simulations is inappropriate, since the lattice simulations are done for full chemical equilibrium. Furthermore, the temperature of freeze-out may be not connected with the phase transition temperature — we expect only that the latter is higher than the former.

It is also worth emphasizing that the case with $\gamma_q \neq 1$ and $\gamma_s \neq 1$ is equivalent to the introduction of the non-equilibrium chemical potentials $\mu_q/T = \ln \gamma_q$ and $\mu_s/T = \ln \gamma_s$ through the relation

$$\Upsilon_i \equiv \exp \left(\frac{\mu_q (N_q^i + N_{\bar{q}}^i) + \mu_s (N_s^i + N_{\bar{s}}^i)}{T} \right). \quad (9)$$

From Eq. (9) one can conclude, for example, that the conditions $\mu_i > 0$ or $\gamma_i > 1$ ($i = q, s$) mean that the number of quark and anti-quark pairs in this case is larger than the corresponding equilibrium number obtained with the same temperature. This kind of phenomenon may appear because of fast expansion and cooling of the strongly interacting system. It can be also a result of the interplay between annihilation and recombination processes and, possibly, QCD mechanisms like the gluon condensation followed by the formation of low momentum $q\bar{q}$ pairs

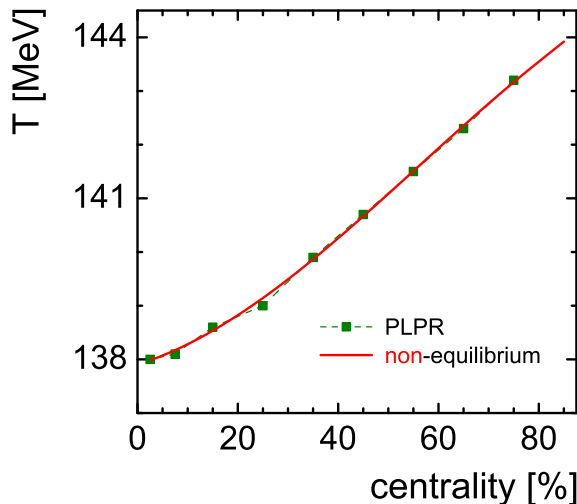


FIG. 1: (Color online) Temperature T shown as a function of centrality for the chemical non-equilibrium model (solid red line). The results from Ref. [29] are denoted as PLPR.

which fuse into pions which subsequently condense [48], see also [49, 50]. Nevertheless, using Eqs. (8) and (9) we imply that there are only two parameters responsible for deviations from the standard statistical model — the corrections for all particles scale in the way corresponding to their quark content.

We note that the value of γ_q used in Ref. [29] is equivalent to the pion chemical potential $\mu_\pi = 2T \ln \gamma_q \simeq 134$ MeV, which is very close to the π^0 mass, $m_{\pi^0} \simeq 134.98$. It may suggest that a substantial part of π^0 mesons form the condensate. Since the prediction of the Bose condensation in 1924 [51, 52] the beauty and simplicity of this phenomenon have attracted attention of many physicists [49, 50, 53–62]. However, only recently it has been confirmed experimentally in the system of cold atoms [63, 64]. The high temperature Bose condensation on the $\text{MeV} \sim 10^{12}\text{K}$ scale is also possible even in very small systems which are created in elementary particle collisions [65]. The Bose condensate formed in the ultra-relativistic regime has been considered in Refs. [66, 67] as a dark matter candidate in cosmological models. There are also interesting effects that appear inside of the pion condensate, see, e.g., Ref. [68]. Besides that, large pion chemical potentials may lead to the formation of other types of condensates like a di-quark Bose condensate [69, 70]. All those findings indicate at the importance of further studies of the Bose condensation phenomenon in high-energy physics.

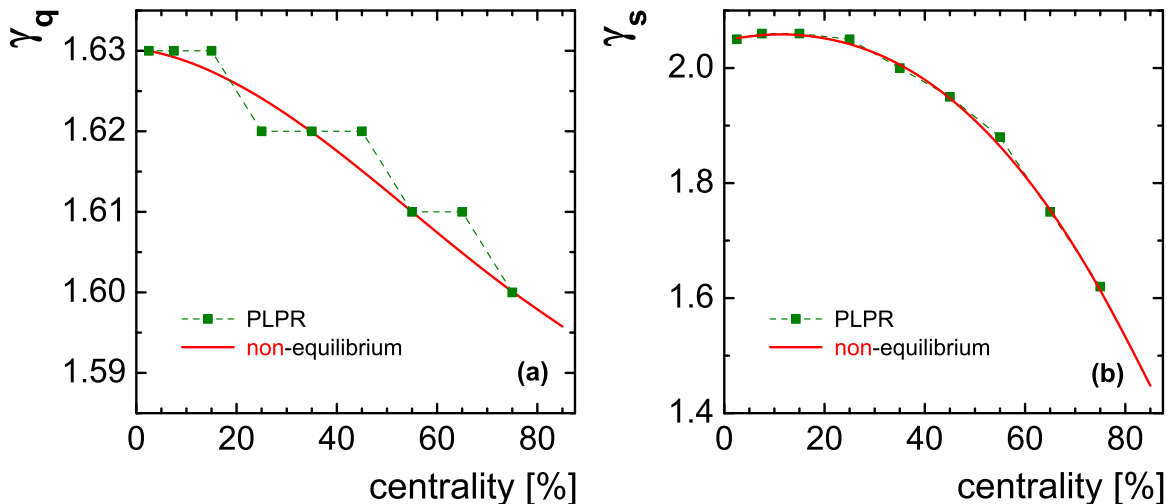


FIG. 2: (Color online) The parameters γ_q (a) and γ_s (b) as functions of centrality for the chemical non-equilibrium model.

III. FIXING MODEL PARAMETERS — SPECTRA OF PIONS AND KAONS

Similarly as in our previous work [36], we use the thermodynamic parameters of the NEQ SHM model determined first in Ref. [29]. In Ref. [36] we used the values of T , γ_q , and γ_s from [29] and determined the values of r_{\max} and τ_f from the χ^2 fit to the spectra of pions and kaons. In this work we adapt a simpler method — in addition to T , γ_q , and γ_s we use also the value of the volume dV/dy determined in [29]. The latter introduces a relation between r_{\max} and τ_f , see Eq. (6), hence, we need to fit only one parameter, which we choose to be the ratio r_{\max}/τ_f . In multiple calculations we have verified that the use of T , γ_q , and γ_s from [29] together with the two-dimensional fit of r_{\max} and τ_f leads to the same results as the use of T , γ_q , γ_s , and dV/dy from [29] along with the one dimensional fit of r_{\max}/τ_f .

In order to analyze the centrality classes different from those studied in Ref. [29] and to facilitate the numerical manipulations, we use polynomial approximations for the functions $T(c)$, $\gamma_q(c)$, $\gamma_s(c)$, and $dV/dy(c)$. They are explicitly given in Appendix B. In practice, for the centrality class defined by the range $c = c_1$ – c_2 %, we use the values from the middle of the range, for example, we take $T((c_1 + c_2)/2)$. Having determined the optimal value of r_{\max}/τ_f for each studied centrality class, we use it to make predictions for the p_T spectra of protons and other hadron species.

In Fig. 1 we show the centrality dependence of the temperature T used in NEQ SHM. The

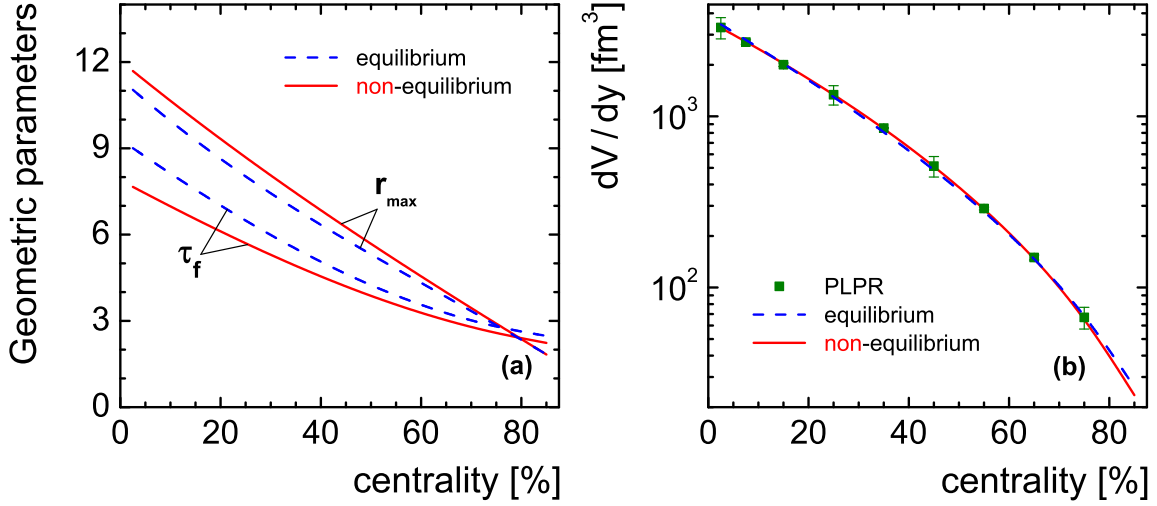


FIG. 3: (Color online) Geometric parameters (a) and the volume per unit rapidity (b) for both the chemical non-equilibrium and chemical equilibrium models.

small squares represent the values taken from Ref. [29], the dashed line (denoted as PLPR) is the interpolation of the results found in Ref. [29], and the red line represents our approximation. In Fig. 2 we show the two analogous plots of $\gamma_q(c)$ and $\gamma_s(c)$ in the (a) and (b) panels, respectively. In Fig. 3 we show the geometric parameters (a) and the volume per unit rapidity (b) for both the chemical non-equilibrium and chemical equilibrium models. In the EQ SHM version we fix the temperature to be the same for all centralities, $T = 165.6$ MeV, and fit both r_{max} and τ_f . In this case, once again we fit first the pion and kaon spectra only, and use the obtained parameters for all other particles. It is interesting to notice that although the geometric parameters are different for NEQ SHM and EQ SHM the volume per unit rapidity remains almost unchanged if we fix the centrality class.

The results of our calculations for pions, $\pi^+ + \pi^-$, kaons, $K^+ + K^-$, and protons, $p + \bar{p}$, are shown in Fig. 4 for NEQ SHM and in Fig. 5 for EQ SHM. We consider all centralities and the whole p_T range provided by the experiment for pions and kaons. In order to show all centralities together we have multiplied each spectrum at a given centrality by the factor displayed in the upper right panel. Experimental error bars in the upper panels are of the size of the symbols and, therefore, they are not shown. The logarithmic scale used for the p_T -axis emphasizes the low p_T region. The lower panels show the data to model ratios for the most central, $c = 0$ –5%, semi-peripheral, $c = 30$ –40%, and ultra-peripheral collisions, $c = 80$ –90%.

In the upper panels of Figs. 4 and 5 one can observe a good agreement for pions and kaons

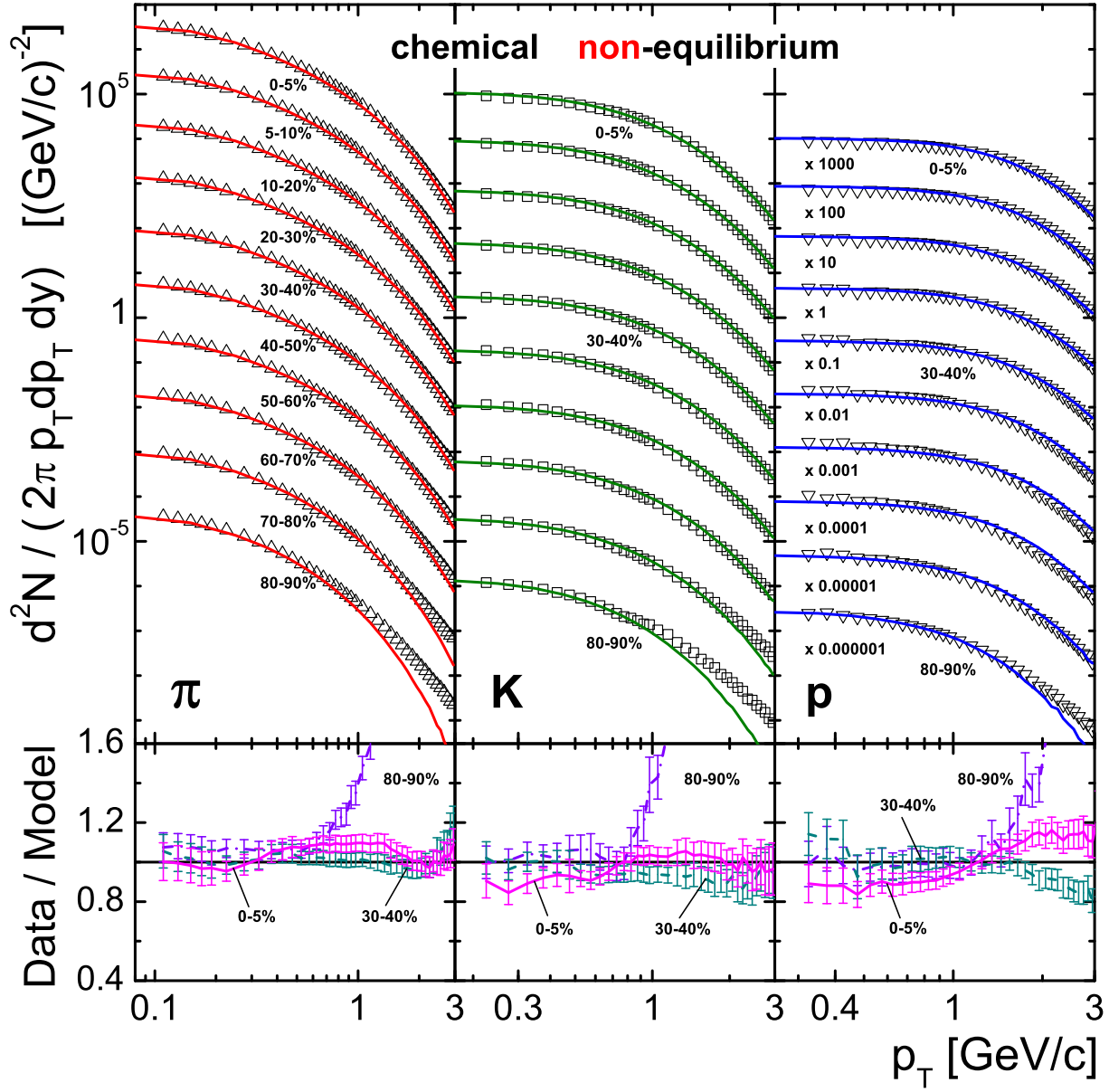


FIG. 4: (Color online) Upper panels: Transverse-momentum spectra of pions (left), kaons (middle) and protons (right) in different centrality classes. The data [23] are shown by the open symbols. The calculations in the non-equilibrium version of the Cracow model are indicated by the lines. Lower panels: The ratios of the experimental and theoretical p_T spectra in the most central ($c = 0-5\%$), semi-peripheral ($c = 30-40\%$) and ultra-peripheral ($c = 80-90\%$) collisions for pions, kaons, and protons.

both for NEQ and EQ versions of the Cracow model in the wide p_T range and for all centralities. This agreement is a strong argument in favor of the parametrization (2) of the flow at freeze-out. On the other hand, the protons in central collisions are described only in NEQ, as we first

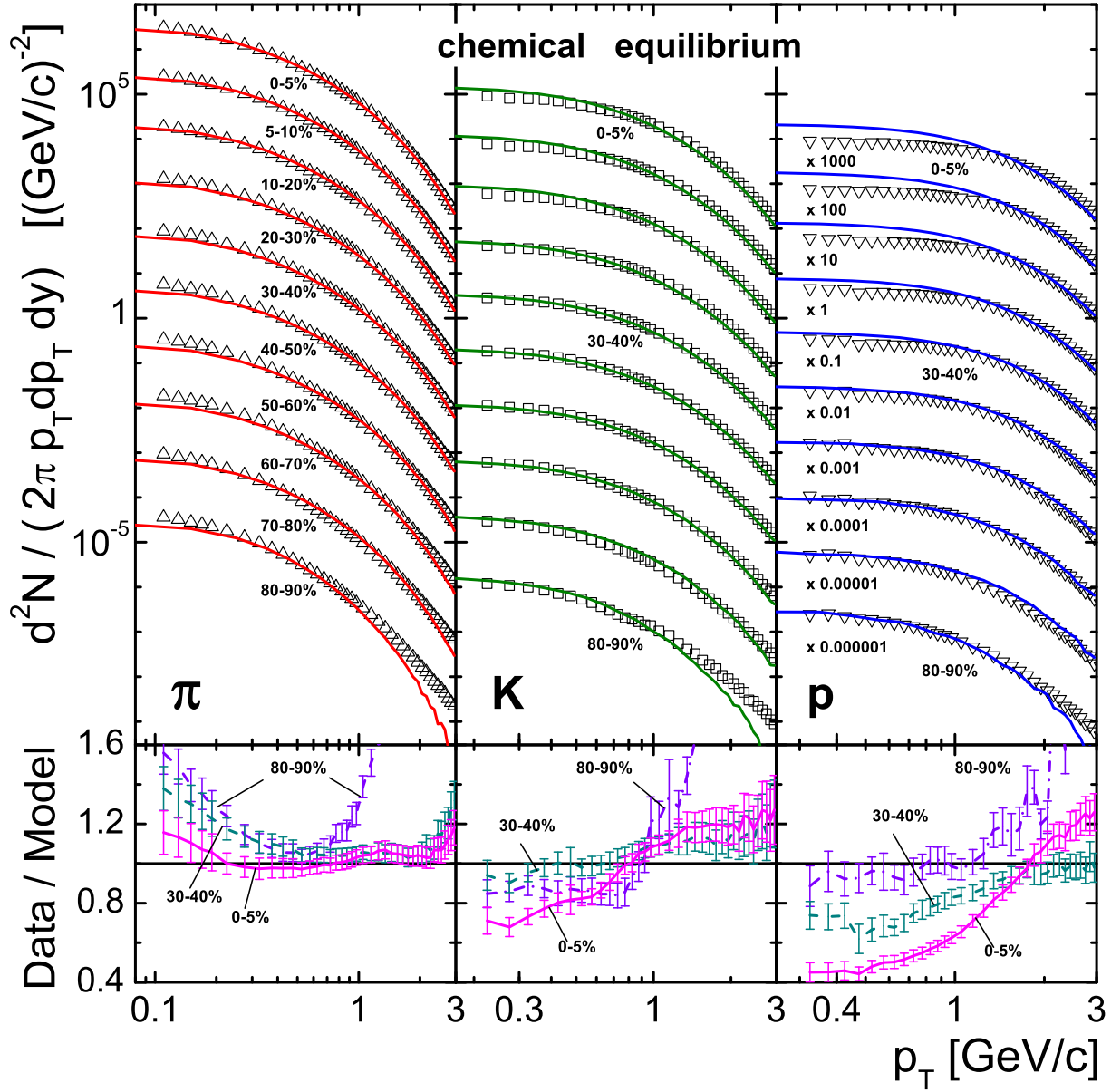


FIG. 5: (Color online) Same as Fig. 4 but in the equilibrium Cracow model.

observed in [36].

The agreement between the data and the model predictions is more clearly displayed in the lower panels of Figs. 4 and 5 where the linear vertical scale is used. The NEQ lines in the Cracow model go exactly through the experimental points for pions and kaons, for most central and semi-peripheral collisions in the whole range from the lowest available point up to $p_T = 3$ GeV. The deviations appear only in ultra-peripheral collisions for $p_T \gtrsim 1.5$ GeV. In spite of the fact that we fitted only pions and kaons, the agreement for protons is also very

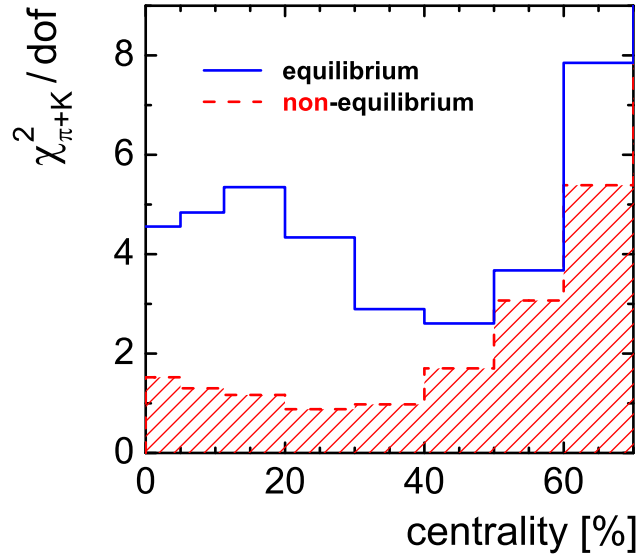


FIG. 6: (Color online) The centrality dependence of the χ^2 calculated for the joint fit of the p_T spectra of pions and kaons.

good.

Comparing Figs. 4 and 5 one can check that the NEQ fit is much better than the EQ fit. Moreover, in EQ SHM the demand of the best fit for pions and kaons bends pions up and kaons down at low p_T . The proton spectra behave similarly to the kaon spectra. The protons are so much in anti-correlation with the pions, that a simultaneous fit of the low p_T part of the spectrum of pions and protons in EQ SHM seems to be impossible.

The quality of the fit in NEQ and EQ is illustrated in Fig. 6. The values of χ^2 indicate that NEQ SHM is three times better for central and semi-central collisions. Starting with the centrality of about 40%, the difference between NEQ and EQ SHM decreases while the values of χ^2 grow very rapidly. This behavior may be explained by the qualitative change of the spectra which are exponential in central and semi-central collisions and become well described by a power law in peripheral collisions.

IV. SPECTRA OF STRANGE PARTICLES

Another challenging test for the NEQ SHM model is a comparison of the model predictions with the data available for the p_T spectra of strange particles. In order to verify the model we use the same parameters as those found in the study of pions and kaons. We do not present here

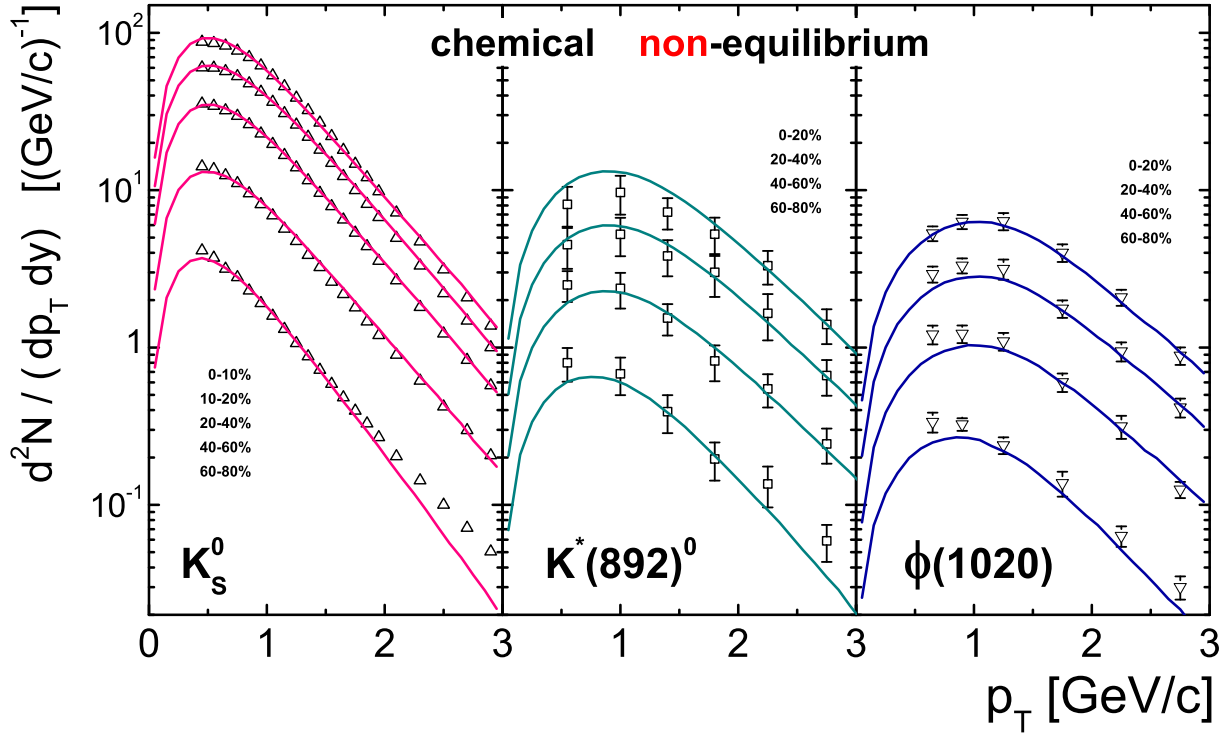


FIG. 7: (Color online) Transverse-momentum spectra of K_S^0 (left), $K^*(892)^0$ (middle) and $\phi(1020)$ (right) in different centrality classes. The data [37, 38] are shown by the open symbols. The calculations in the non-equilibrium Cracow model are indicated by the lines.

the results for the chemical equilibrium version, since it always yields much worse agreement with the data as compared to the chemical non-equilibrium version.

In the model analysis of the spectra of strange particles it is very important to take into account the same weak decay corrections as those considered by the experiment. The ALICE Collaboration does not specify the weak corrections for K_S^0 , hence, we take into account the K_S^0 's coming from all possible decays. The spectra of the Λ hyperons were corrected for the feed-down contributions coming from the weak decays of Ξ^- and Ξ^0 . Therefore, we subtract the feed-down from these particles only. ALICE also did not correct the Λ spectra for the feed-down from non-weak decays of Σ^0 and from the $\Sigma(1385)$ family. All Σ^0 and 88.25% of $\Sigma^-(1385)$, $\Sigma^0(1385)$ and $\Sigma^+(1385)$ decay into Λ , therefore, we include all of them in the Λ yield. The Ξ 's and Ω 's are directly taken from the generated events.

The results for K_S^0 , $K^*(892)^0$ and $\phi(1020)$ are shown in Fig. 7. The error bars are indicated only if they are bigger than the corresponding symbols in the figure. One can see that the p_T spectra of these particles are fitted very well. For many centralities the NEQ model lines

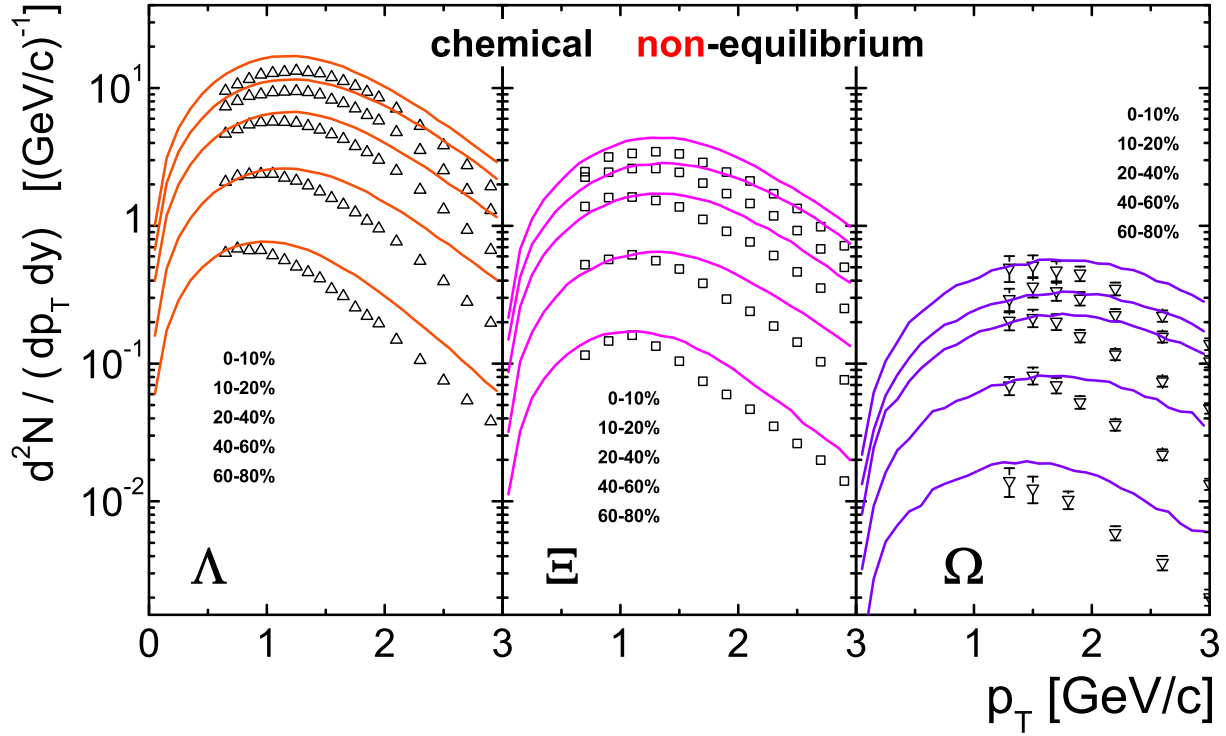


FIG. 8: (Color online) The same as in Fig. 7 but for Λ [37], Ξ and Ω [39].

go through the experimental points. We stress that it is very nontrivial that the fit done initially for $\pi^+ + \pi^-$ and $K^+ + K^-$ only appears so good also for $p + \bar{p}$, K_S^0 , $K^*(892)^0$ and $\phi(1020)$. These particles have a different quark content and therefore different non-equilibrium corrections according to Eq. (8). Moreover, the $K^*(892)^0$, in contrast to other particles, is a short living resonance that could interact frequently with the hadronic matter possibly formed in the final state. The fact that we fit its spectrum together with the long living $\phi(1020)$ supports our picture of the non-equilibrium hadronization and the single freeze-out.

The model and experimental p_T spectra of the hyperons (Λ , $\Xi = \Xi^+ + \Xi^-$, and $\Omega = \Omega^+ + \Omega^-$) are shown in Fig. 8. One can see that the experimental results at low p_T are reproduced, but for higher values of p_T ($p_T > 2$ GeV) the NEQ SHM overshoots the data. Such deviations increase for heavier particles. On one hand, we expect that our model's predictions may break down at large values of the transverse momentum, on the other hand, the observed differences can be an artefact of the Cracow model that assumes a simple Hubble form of flow at freeze-out for all particles, see Eq. (2). Thus, the excess at high p_T may be an indication that heavy particles

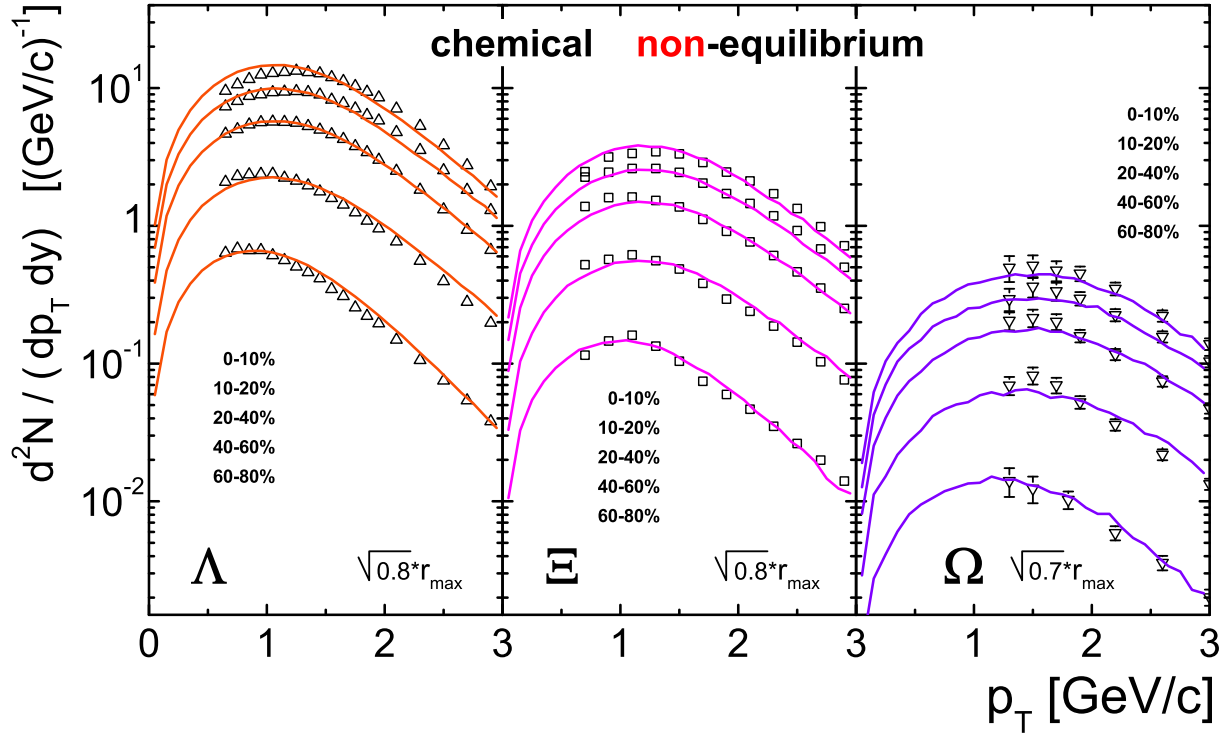


FIG. 9: (Color online) The same as in Fig. 8 but assuming the emission of Λ , Ξ and Ω from the inner part of the system, see text for details.

in our model experience too much flow ⁴.

We have checked, that one can improve the agreement between the model predictions and the data by using the same freeze-out time and choosing a different maximum radius of the firecylinder for heavy strange particles. It changes their multiplicity which is proportional to the volume $dV/dy \sim r_{\max}^2$ and the shape of the spectrum, that is sensitive to the ratio r_{\max}/τ_f . The assumption of a smaller emission volume for Λ 's and Ξ 's (by 20%) and also for Ω 's (by 30%) gives us a remarkable agreement, see Fig. 9. With the reduced r_{\max} and other parameters unchanged, the model results agree with the experimental points even for Ω 's measured at the highest measured centrality. To some extent, such an approach reminds the recent proposal of a two step freeze-out [72].

Altogether, our results lead to the freeze-out picture shown in Fig. 10. In the center-of-mass frame at $z = 0$, the freeze-out starts in the center of the fireball at the time τ_f . Subsequently,

⁴ A similar conclusion was drawn from the blast wave fits presented in Ref. [71]

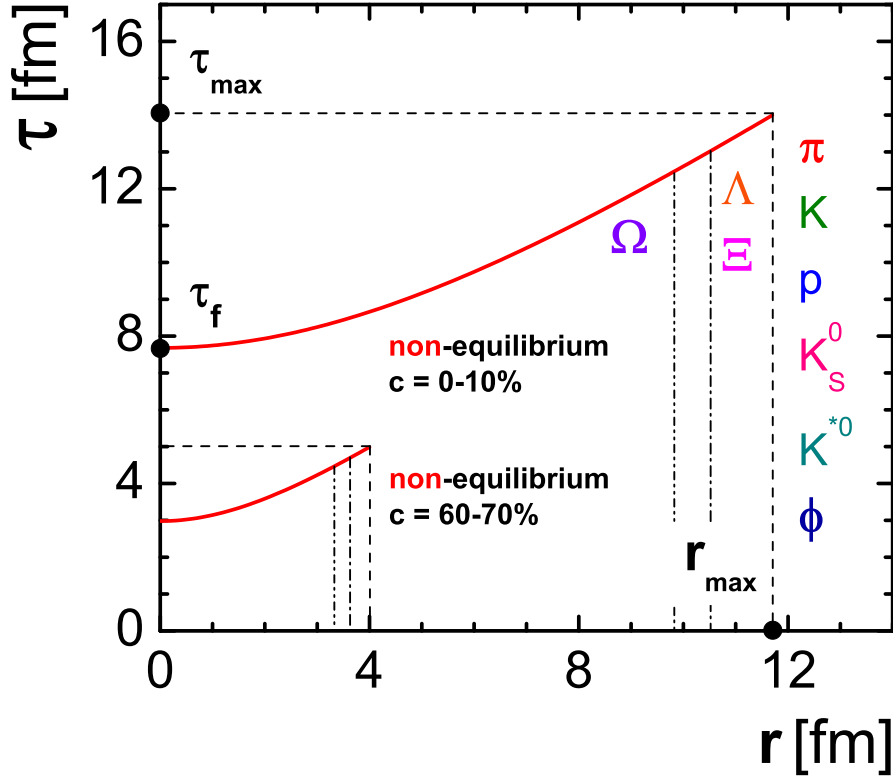


FIG. 10: (Color online) The freeze-out line in the non-equilibrium Cracow model.

it spreads out along the hyperbola [40, 41]

$$\tau(r) = \sqrt{\tau_f^2 + r^2} \leq \sqrt{\tau_f^2 + r_{\max}^2}. \quad (10)$$

The radius $r = \sqrt{0.7} r_{\max}$ ($r = \sqrt{0.8} r_{\max}$) determines the production range for Ω 's and Ξ 's (Λ 's). All other particles are produced in the range ending at $r = r_{\max}$.

V. CONCLUSIONS

In this work we have analyzed the transverse-momentum spectra of strange hadrons produced in Pb+Pb collisions at the collision energy $\sqrt{s_{\text{NN}}} = 2.76$ TeV. In this way, we have extended our approach initiated in Ref. [36] where we studied pions, kaons, and protons, only. An additional new aspect of the present work is the complete analysis of the data collected at different centrality classes.

Our approach combines the concept of chemical non-equilibrium with the single-freeze-out scenario. To calculate the transverse-momentum spectra we have used the framework of the Cracow model with thermodynamic parameters established in earlier studies of the ratios of

	Non-Equilibrium					Equilibrium	
	r_{\max}	τ_f	T	γ_q	γ_s	r_{\max}	τ_f
A	12.046	7.89	137.91	1.63	2.05	11.42	9.31
B	$-1.44 \cdot 10^{-1}$	$-9.34 \cdot 10^{-2}$	$2.57 \cdot 10^{-5}$	$-6.17 \cdot 10^{-5}$	$2.05 \cdot 10^{-3}$	$-1.57 \cdot 10^{-1}$	$-1.22 \cdot 10^{-1}$
C	$3.97 \cdot 10^{-4}$	$1.65 \cdot 10^{-4}$	$1.08 \cdot 10^{-6}$	$-8.34 \cdot 10^{-6}$	$-7.69 \cdot 10^{-5}$	$9.47 \cdot 10^{-4}$	$2.90 \cdot 10^{-4}$
D	$-1.40 \cdot 10^{-6}$	$1.77 \cdot 10^{-6}$	$-6.42 \cdot 10^{-9}$	$5.05 \cdot 10^{-8}$	$-3.56 \cdot 10^{-7}$	$-4.98 \cdot 10^{-6}$	$2.36 \cdot 10^{-6}$

TABLE I: Coefficients used in Eq. (B1) describing the centrality dependence of the thermodynamic and geometric parameters for the two versions of the model.

hadron abundances. The geometric parameters of the model have been obtained from the fit to the pion and kaon spectra. Using the same thermodynamic and geometric parameters, we have obtained an excellent description of the spectra of K_S^0 's, $K^*(892)^0$'s, and $\phi(1020)$'s. These particles have different lifetimes, and the presence of a long hadronic phase after the chemical freeze-out would change the temperature parameters characterizing $K^*(892)^0$'s and $\phi(1020)$'s. Therefore, our simultaneous description of $K^*(892)^0$'s and $\phi(1020)$'s confirms the validity of the single-freeze-out approximation. A satisfactory description is also obtained for Λ , Ξ and Ω in the low p_T region. Further improvement of the hyperon spectra may be achieved if we assume that they are emitted from a smaller, internal part of the system but still at the same thermodynamic conditions.

Our general conclusion is that the chemical non-equilibrium model with essentially one extra geometric parameter allows for a very good description of the spectra of all measured hadrons in heavy-ion collisions at the LHC energies. Since at lower energies the spectra were very well described by the equilibrium model with $\gamma_q = 1$ [43], it may suggest a new physics mechanism of particle production at the LHC.

Acknowledgments

V.B and W.F. were supported by Polish National Science Center grant No. DEC-2012/06/A/ST2/00390. M.R. was supported in part by Polish National Science Center grant No. DEC-2011/01/D/ST2/00772.

Appendix A: Rapidity and spacetime rapidity distributions

Using our definition of the element of the freeze-out hypersurface $d\Sigma_\mu$ in (1) we may write

$$E \frac{dN}{d^3p} = \tau_f \int_0^{r_{\max}} r dr \int_{-\infty}^{+\infty} d\eta \int_0^{2\pi} d\varphi p \cdot u f(p \cdot u). \quad (\text{A1})$$

Integrating this equation over momentum gives

$$\frac{dN}{d\eta} = \tau_f \int_0^{r_{\max}} r dr \int_0^{2\pi} d\varphi u_\mu \int \frac{d^3p}{E} p^\mu f(p \cdot u). \quad (\text{A2})$$

The covariant form of the last integral on the right-hand side in (A2) implies

$$\frac{dN}{d\eta} = \tau_f \int_0^{r_{\max}} r dr \int_0^{2\pi} d\varphi n(T, \Upsilon). \quad (\text{A3})$$

If the freeze-out conditions correspond to constant values of T and Υ , the last factor in (A3) factorizes and we obtain the desired formula

$$\frac{dN}{d\eta} = \pi r_{\max}^2 \tau_f n(T, \Upsilon). \quad (\text{A4})$$

In addition, the boost invariance of Eq. (A1) implies that the density $dN/d\eta$ is obtained from the expression whose general form may be written as

$$\frac{dN}{d\eta} = \int dy \int d^2p_T F(p_T, y - \eta), \quad (\text{A5})$$

where F is a function of the difference $y - \eta$. From Eq. (A5) we conclude that

$$\frac{dN}{d\eta} = \frac{dN}{dy}. \quad (\text{A6})$$

Appendix B: Thermodynamic parameters as functions of centrality

In this Section we present our approximate formulas for the centrality dependence of the thermodynamic and geometric parameters in the chemical non-equilibrium and chemical equilibrium models. All functions are approximated by the third-order polynomial of the form

$$A + Bc + Cc^2 + Dc^3, \quad (\text{B1})$$

where c is given in percentages multiplied by 100. The appropriate coefficients are given in Table I.

[1] P. Koch, J. Rafelski, South Afr. J. Phys. **9**, 8 (1986).

- [2] J. Cleymans, H. Satz, Z. Phys. C **57**, 135 (1993).
- [3] J. Cleymans, K. Redlich, Phys. Rev. Lett. **81**, 5284 (1998).
- [4] M. Gazdzicki, M. I. Gorenstein, Acta Phys. Polon. B **30**, 2705 (1999).
- [5] P. Braun-Munzinger, J. Stachel, J. P. Wessels, N. Xu, Phys. Lett. B **344**, 43 (1995).
- [6] J. Cleymans, D. Elliott, H. Satz, R. L. Thews, Z. Phys. C **74**, 319 (1997).
- [7] F. Becattini, J. Cleymans, A. Keranen, E. Suhonen, K. Redlich, Phys. Rev. C **64**, 024901 (2001).
- [8] J. Sollfrank, M. Gazdzicki, U. W. Heinz, J. Rafelski, Z. Phys. C **61**, 659 (1994).
- [9] E. Schnedermann, J. Sollfrank, U. W. Heinz, Phys. Rev. C **48**, 2462 (1993).
- [10] P. Braun-Munzinger, J. Stachel, J. P. Wessels, N. Xu, Phys. Lett. B **365**, 1 (1996).
- [11] F. Becattini, J. Phys. G **23**, 1933 (1997).
- [12] G. D. Yen, M. I. Gorenstein, Phys. Rev. C **59**, 2788 (1999).
- [13] P. Braun-Munzinger, I. Heppe, J. Stachel, Phys. Lett. B **465**, 15 (1999).
- [14] F. Becattini, M. Gazdzicki, A. Keranen, J. Manninen, R. Stock, Phys. Rev. C **69**, 024905 (2004).
- [15] P. Braun-Munzinger, D. Magestro, K. Redlich, J. Stachel, Phys. Lett. B **518**, 41 (2001).
- [16] W. Florkowski, W. Broniowski, M. Michalec, Acta Phys. Polon. B **33**, 761 (2002).
- [17] W. Broniowski, W. Florkowski, Phys. Rev. Lett. **87**, 272302 (2001).
- [18] W. Broniowski, W. Florkowski, Phys. Rev. C **65**, 064905 (2002).
- [19] W. Broniowski, A. Baran and W. Florkowski, AIP Conf. Proc. **660**, 185 (2003).
- [20] F. Retiere, M. A. Lisa, Phys. Rev. C **70**, 044907 (2004).
- [21] W. Florkowski, “Phenomenology of Ultra-Relativistic Heavy-Ion Collisions,” (World Scientific, Singapore, 2010).
- [22] B. Abelev *et al.* [ALICE Collaboration], Phys. Rev. Lett. **109**, 252301 (2012).
- [23] B. Abelev *et al.* [ALICE Collaboration], Phys. Rev. C **88**, 044910 (2013).
- [24] J. Stachel, A. Andronic, P. Braun-Munzinger and K. Redlich, arXiv:1311.4662 [nucl-th].
- [25] M. Rybczynski, W. Florkowski and W. Broniowski, Phys. Rev. C **85**, 054907 (2012).
- [26] J. Steinheimer, J. Aichelin and M. Bleicher, Phys. Rev. Lett. **110**, 042501 (2013).
- [27] F. Becattini, M. Bleicher, T. Kollegger, T. Schuster, J. Steinheimer and R. Stock, Phys. Rev. Lett. **111**, 082302 (2013).
- [28] M. Petran and J. Rafelski, Phys. Rev. C **88**, no. 2, 021901 (2013)
- [29] M. Petran, J. Letessier, V. Petracek and J. Rafelski, Phys. Rev. C **88**, 034907 (2013).
- [30] H. Song, S. Bass and U. W. Heinz, Phys. Rev. C **89**, 034919 (2014).

- [31] I. A. Karpenko, Y. M. Sinyukov and K. Werner, Phys. Rev. C **87**, 024914 (2013).
- [32] K. Werner, I. Karpenko, M. Bleicher, T. Pierog and S. Porteboeuf-Houssais, Phys. Rev. C **85**, 064907 (2012).
- [33] P. Bozek and I. Wyskiel-Piekarska, Phys. Rev. C **85**, 064915 (2012).
- [34] L. Pang, Q. Wang and X. -N. Wang, arXiv:1309.6735 [nucl-th].
- [35] C. Gale, S. Jeon, B. Schenke, P. Tribedy and R. Venugopalan, Phys. Rev. Lett. **110**, 012302 (2013).
- [36] V. Begun, W. Florkowski and M. Rybczynski, arXiv:1312.1487 [nucl-th].
- [37] B. B. Abelev *et al.* [ALICE Collaboration], Phys. Rev. Lett. **111**, 222301 (2013).
- [38] B. B. Abelev *et al.* [ALICE Collaboration], arXiv:1404.0495 [nucl-ex].
- [39] B. B. Abelev *et al.* [ALICE Collaboration], Phys. Lett. B **728**, 216 (2014).
- [40] A. Kisiel, T. Taluc, W. Broniowski and W. Florkowski, Comput. Phys. Commun. **174**, 669 (2006).
- [41] M. Chojnacki, A. Kisiel, W. Florkowski and W. Broniowski, Comput. Phys. Commun. **183**, 746 (2012).
- [42] G. Torrieri, S. Steinke, W. Broniowski, W. Florkowski, J. Letessier and J. Rafelski, Comput. Phys. Commun. **167**, 229 (2005).
- [43] D. Prorok, Phys. Rev. C **75**, 014903 (2007).
- [44] F. Becattini, M. Bleicher, T. Kollegger, M. Mitrovski, T. Schuster and R. Stock, Phys. Rev. C **85**, 044921 (2012).
- [45] F. Becattini and J. Manninen, J. Phys. G **35**, 104013 (2008).
- [46] F. Becattini and J. Manninen, Phys. Lett. B **673**, 19 (2009).
- [47] P. Bozek, Acta Phys. Polon. B **36**, 3071 (2005).
- [48] J. Letessier and J. Rafelski, Phys. Rev. C **59**, 947 (1999).
- [49] J. -P. Blaizot, F. Gelis, J. -F. Liao, L. McLerran and R. Venugopalan, Nucl. Phys. A **873**, 68 (2012).
- [50] J. -P. Blaizot, J. Liao and L. McLerran, Nucl. Phys. A **920**, 58 (2013).
- [51] S. N. Bose, Z. Phys. **26**, 178 (1924).
- [52] A. Einstein, Sitz. Ber. Preuss. Akad. Wiss. (Berlin) **1**, 3 (1925).
- [53] J. Zimanyi, G. I. Fai and B. Jakobsson, Phys. Rev. Lett. **43**, 1705 (1979).
- [54] I. N. Mishustin, L. M. Satarov, J. Maruhn, H. Stoecker and W. Greiner, Phys. Lett. B **276**, 403 (1992).

- [55] C. Greiner, C. Gong and B. Muller, Phys. Lett. B **316**, 226 (1993).
- [56] S. Pratt, Phys. Lett. B **301**, 159 (1993).
- [57] W. Florkowski and M. Abu-Samreh, Z. Phys. C **70**, 133 (1996).
- [58] T. Csorgo and J. Zimanyi, Phys. Rev. Lett. **80**, 916 (1998).
- [59] A. Bialas and K. Zalewski, Phys. Lett. B **436**, 153 (1998).
- [60] R. Lednicky, V. Lyuboshitz, K. Mikhailov, Y. Sinyukov, A. Stavinsky and B. Erasmus, Phys. Rev. C **61**, 034901 (2000).
- [61] V. V. Begun and M. I. Gorenstein, Phys. Lett. B **653**, 190 (2007).
- [62] E. Kokoulina [SVD-2 Collaboration], PoS ICHEP **2012**, 259 (2013).
- [63] M. H. Anderson, J. R. Ensher, M. R. Matthews, C. E. Wieman and E. A. Cornell, Science **269**, 198 (1995).
- [64] K. B. Davis, M. -O. Mewes, M. R. Andrews, N. J. van Druten, D. S. Durfee, D. M. Kurn and W. Ketterle, Phys. Rev. Lett. **75**, 3969 (1995).
- [65] V. V. Begun and M. I. Gorenstein, Phys. Rev. C **77**, 064903 (2008).
- [66] J. Madsen, Phys. Rev. Lett. **69**, 571 (1992).
- [67] D. Boyanovsky, H. J. de Vega and N. Sanchez, Phys. Rev. D **77**, 043518 (2008).
- [68] T. Kalaydzhyan, Phys. Rev. D **89**, 105012 (2014).
- [69] R. Rapp, T. Schäfer, E. V. Shuryak and M. Velkovsky, Phys. Rev. Lett. **81**, 53 (1998).
- [70] K. Splittorff, D. T. Son and M. A. Stephanov, Phys. Rev. D **64**, 016003 (2001).
- [71] I. Melo, B. Tomasik, poster presentation at the *Quark Matter 2014* conference, Darmstadt, Germany, 2014.
- [72] S. Chatterjee, R. M. Godbole and S. Gupta, Phys. Lett. B **727**, 554 (2013).